Carbohydrate Polymers 111 (2014) 633–644

Contents lists available at ScienceDirect

Carbohydrate Polymers

journal homepage: www.elsevier.com/locate/carbpol

Mekabu fucoidan: Structural complexity and defensive effects against avian influenza A viruses

Andriy Synytsya[a,*], Roman Bleha[a], Alla Synytsya[b], Radek Pohl[c], Kyoko Hayashi[d], Keiko Yoshinaga[e], Takahisa Nakano[e], Toshimitsu Hayashi[f]

[a] Department of Carbohydrates and Cereals, Institute of Chemical Technology in Prague, Technická 5, 166 28 Prague 6, Czech Republic
[b] Department of Analytical Chemistry, Institute of Chemical Technology in Prague, Technická 5, 166 28 Prague 6, Czech Republic
[c] Institute of Organic Chemistry and Biochemistry AS CR, Flemingovo sq. 2, 166 28 Prague 6, Czech Republic
[d] Graduate School of Medicine and Pharmaceutical Sciences for Research, University of Toyama, 2630 Sugitani, Toyama 930-0194, Japan
[e] Riken Vitamin Co., Ltd., 2-9-18 Misaki-cho, Chiyoda-ku, Tokyo 101-8370, Japan
[f] Research Institute of Life and Health Sciences, Chubu University, 1200 Matsumoto-cho, Kasugai, Aichi 487-8501, Japan

ARTICLE INFO

Article history:
Received 13 February 2014
Received in revised form 6 May 2014
Accepted 8 May 2014
Available online 23 May 2014

Keywords:
Mekabu fucoidan
Sporophyll *Undaria pinnatifida*
Spectroscopic methods
Avian influenza A virus
Immunostimulating effect

ABSTRACT

Fucoidan from the sporophyll (Mekabu) of brown seaweed *Undaria pinnatifida* (wakame) is interesting due to its various biological activities. Mekabu fucoidan (M_w ~9 kDa) of this study (MF) was previously isolated and characterized by chemical and separation methods including GPC and methylation analysis (Lee, Hayashi, Hashimoto, Nakano, & Hayashi, 2004). It was found that this fucoidan composed of partially sulphated (*DS* ~0.72) fucose and galactose at approximately equal amounts. Methylation analyses revealed complex structure of MF. However, it has been still unclear about the linkages between units and substitution patterns. To solve these structural tasks, spectroscopic methods (FTIR, FT Raman and NMR) were used in the analysis of native MF and its deesterified derivatives. According to obtained results, this polysaccharide was defined as *O*-acetylated sulphated fucogalactan. The defensive effects of MF were evaluated on mice infected with avian influenza A viruses (H5N3 and H7N2 subtypes); its efficacy was determined in reducing viral replication and increasing antibody production. Oral administration of MF resulted in suppressing virus yields. In addition, the production of neutralizing antibodies and mucosal IgA in the animals inoculated with the avian influenza A viruses was significantly increased. These results suggested that MF could be used for the prevention of viral infection.

1. Introduction

Brown alga wakame (*Undaria pinnatifida*) has been traditionally used for preparation of healthy food products in Japan and other countries of East Asia (Taboada, Millán, & Miguez, 2013). This alga is rich of minerals, vitamins, dietary fibres and many other compounds maintaining human health. Partially, its sporophyll (Mekabu) contains polysaccharide fucoidan, which is interesting due to its anticoagulant, immunomodulation, antiviral, antiprotozoal and many other biological activities (Fitton, 2011; Maruyama, Tanaka, Hashimoto, Inoue, & Sasahara, 2007). Fucoidan from *U. pinnatifida* induced apoptosis in various cancer cells via the ROS-mediated mitochondrial pathway (Yang et al., 2013) or through down-regulation of p38, PI3K/Akt and the activation of the ERK1/2 MAPK pathway (Boo et al., 2011). This polysaccharide modulates Th2 responses and thus might be useful for treating allergic inflammation (Maruyama, Tamauchi, Hashimoto, & Nakano, 2005) and mediates tumour destruction through responses of Th1 and NK cells (Maruyama, Tamauchi, Hashimoto, & Nakano, 2003; Maruyama, Tamauchi, Iizuka, & Nakano, 2006). It is less cytotoxic to immune cells than common fucoidan from *Fucus vesiculosis*, and possesses immunomodulating activity to produce cytokines and chemokines from macrophages and splenocytes (Yoo et al., 2007). Mekabu fucoidan showed potential antiviral activities against herpes simplex viruses, human cytomegalovirus and influenza A virus (Hayashi, Lee, Nakano, & Hayashi, 2013; Hemmingson, Falshaw, Furneaux, & Thompson, 2006; Lee et al., 2004). Intake of Mekabu fucoidan was found to increase antibody production in the immunocompromised persons in a randomized, placebo-controlled, double-blind study after influenza vaccination in elderly Japanese men and women (Negishi, Mori, Mori, & Yamori, 2013). This fucoidan also supresses angiogenesis (Liu et al., 2012), demonstrates antioxidant properties (Mak, Hamid, Liu, Lu, & White, 2013) and selectively inhibits several key enzymes including secretory phospholipase A2-IIA, A-kinase and hyaluronidase (Katsube, Yamasaki, Iwamoto, & Oka, 2003; Maruyama, Suzuki, Miyai, &

* Corresponding author. Tel.: +420 220 443 116; fax: +420 220 445 130.
E-mail addresses: sinicaa@vscht.cz, andrej.sinica@vscht.cz (A. Synytsya).

http://dx.doi.org/10.1016/j.carbpol.2014.05.032
0144-8617/

Ohtsuki, 2008). Yang et al. (2008) suggested that anticancer activity of Mekabu fucoidan could be significantly enhanced by partial depolymerisation at mild condition. It has been also reported that such low molecular weight fucoidan suppresses inflammation by promoting the inhibition of mitogen-activated protein kinases and oxidative stress (Kim, Yoon, & Lee, 2012). Oligosaccharides obtained by partial enzymatic hydrolysis of Mekabu fucoidan have exerted strong anticoagulant activities by prolongation of activated partial thromboplastin time (APTT) and thrombin time (TT) (Kim et al., 2010).

Influenza epidemics cause numerous deaths and millions of hospitalizations, but the most frightening effects are seen when new strains of the virus emerge, causing worldwide outbreaks of infection (World Health Organization, 2010). Avian influenza is now widespread among poultry and migratory birds in many countries in Southeast Asia and has been detected in Africa and several European countries (World Health Organization, 2013a, 2013b). Defence against influenza infection involves innate and adaptive immune responses. In the previous studies, we have reported that oral administration of the Mekabu fucoidan enhanced innate and adaptive immunities in the host (Hayashi et al., 2013, 2007; Hayashi, Nakano, Hashimoto, Kanekiyo, & Hayashi, 2008). The consumption of the fucoidan has enhanced activity of phagocytic cells, and also improves the function of natural killer (NK) cells (Hayashi et al., 2008). Moreover, adaptive immunity is stimulated as judged from the increase in virus-specific antibody production in mucosa and blood (Hayashi et al., 2013). In addition, sulphated polysaccharides have generally been evaluated as antiviral substances (Ghosh et al., 2009). Therefore, the fucoidan is suggested to be effective in the prevention of influenza virus.

Resent investigations confirmed (Ghosh et al., 2009) that antiviral activities of sulphated polysaccharides depend not only on their chain length and charge density, but also on their specific structural features like branching, sulphation and/or acetylation patterns etc. Unfortunately, the structure of Mekabu fucoidan is still poorly investigated. Fucoidan yield and composition significantly varied with sporophyll maturation (Mak et al., 2013) and cultivation forms (Lee, Lim, Lee, & Park, 2006) of *U. pinnatifida*. In contrast to common fucoidans, this polysaccharide consists mainly of fucose and galactose at various ratios, i.e. it is galactofucan. In addition, two types of acidic groups, i.e. sulphate and acetic acid, were found to be attached to fucose and/or galactose units as fucosyl (galactosyl) esters (Synytsya et al., 2010). The molecular weight and degrees of substitution (sulphatation and *O*-acetylation) are very variable (Hemmingson et al., 2006). Methylation analysis of several preparations confirmed that this polysaccharide has complex structure with various sugar linkages and sulphate substitution patterns (Hemmingson et al., 2006; Lee et al., 2004). However, relationship between the galactan and fucan parts in whole polysaccharide as well as the distribution of sulphate and acetyl groups are still unclear and need more investigation. Spectroscopic methods (FTIR, FT Raman and NMR) have been successfully used in structural analysis of fucoidans (Bilan et al., 2010, 2004, 2002; Pielesz, Biniaś, & Paluch, 2011; Synytsya et al., 2010), and thus these methods are valuable for this purpose.

This work is devoted to structural analysis of the native Mekabu fucoidan and its desulphated and/or deacetylated derivatives by the use of vibration spectroscopy (FT Raman, FTIR) and correlation NMR experiments. This polysaccharide (M_w ~9 kDa) was previously isolated and characterized by chemical and separation methods including GPC and methylation analysis of native and desulphated forms (Lee et al., 2004). However, the used methods were not sufficient to describe its exact structure. The main task of the present work is to determine anomeric configuration and specific substitution of the structural patterns, i.e. fucose and/or galactose units, and confirm glycosidic connections between them. In this work we also investigated the effects of the Mekabu fucoidan on the viral replication and immune responses induced by avian influenza viruses (H5N3 and H7N2 subtypes) in animals.

2. Experimental

2.1. Extraction and purification of fucoidan

Crude fucoidan was isolated from raw material (sporophyll of *U. pinnatifida*) and then purified according to Lee et al. (2004). Previously raw material was homogenized and defatted by ethanol refluxed at 80 °C for 2 h; then polysaccharide was extracted with 0.15 mol l^{-1} HCl. The extract was neutralized, applied to ultrafiltration and then concentrated. The crude polysaccharide was precipitated from concentrated extract by an excess of ethanol, washed and dried. Purification of the fucoidan was made by the subsequent use of DEAE Toyopearl 650 M, Q-Sepharose FF and Sephacryl S300 HR columns. Fractions were collected and checked by the phenol–H_2SO_4 reagent. Most abundant fractions were selected and each case and used for further purification. Finally purified colourless polysaccharide was dialyzed and lyophilized.

2.2. Deacetylation and desulphation of fucoidan

The purified native fucoidan (**MF**) was treated with aqueous ammonia at 37 °C to remove *O*-acetyl groups (Chizhov et al., 1999). Desulphation of **MF** was performed by the solvolytic method (Lee et al., 2004; Nagasawa, Inoue, & Kamata, 1977). Briefly, the sample of fucoidan was passed through Dowex 50 Wx 8 column (H^+ form) with H_2O. After neutralization with pyridine, the solution was lyophilized. The resulting pyridinium salt of fucoidan was dissolved in 10% methanol/DMSO mixture and then incubated at 80 °C for 5 h with continuous stirring. The solution was dialyzed against distilled water and then lyophilized. Obtained deacetylated and desulphated derivatives of **MF** were assigned as **DA-MF** and **DS-MF**, respectively.

2.3. Spectroscopic measurements

FTIR spectra (spectral region 4000–400 cm^{-1}, 64 scans, resolution 2 cm^{-1}) of the fucoidan samples were recorded in the form of KBr tablets on Nicolet 6700 spectrometer (Thermo Scientific, USA) using Omnic 8.0 software. FT Raman spectra (spectral region 4000–100 cm^{-1}, 256 scans, resolution 2 cm^{-1}) of the samples were recorded with Bruker FT Raman (FRA 106/S, Equinox 55/S) spectrometer equipped with Nd:YAG laser (excitation line 1064 nm, laser power 100 mW), quartz beam splitter and Ge detector (cooled with liquid N_2). Obtained spectra were exported to Origin 6.0 (Microcal Origin, USA) software in CSV or TXT format, where they were 10-point filtered and baseline corrected. The second derivative algorithm was used for analysis of overlapped bands. Peak decomposition of FTIR spectra (783–883 cm^{-1}, multiple Voigt functions) was made using peak fitting module of Origin 6.0 (Microcal Origin, USA) software. Areas of the Voigt components were used for calculation of the relationship between specific sulphate esters in fucoidan.

^1H and ^{13}C NMR spectra of native and modified fucoidans were recorded on Bruker Avance 600 and Bruker Avance 500 in D_2O solutions. Working frequencies were 600.1 MHz and 499.8 MHz for ^1H, 150.9 MHz and 125.7 MHz for ^{13}C, respectively. Correlation spectroscopic ^1H, ^1H-PFG-COSY, ^1H-PFG-TOCSY, ^1H-PFG-ROESY, ^1H, ^{13}C-HSQC and ^1H, ^{13}C-HMBC experiments were applied for resolution and assignment of resonance signals.

2.4. Cell and viruses

Avian influenza viruses, A/duck/313/4/78 (H5N3) and A/duck/47/5/76 (H7N2), were obtained from Dr. Takashi Suzuki at University of Shizuoka, and propagated on Madin-Darby canine kidney (MDCK) cells grown in Eagle's minimum essential medium (MEM) containing 5% foetal bovine serum. For enzyme-linked immunosorbent assay (ELISA), the viruses were purified from the culture medium of infected MDCK cells and plaque assay was performed on the monolayers of these cells as described elsewhere (Hayashi et al., 2013).

2.5. Influenza virus infection in mice

Female specific pathogen-free BALB/c mice weighing between 16 g and 18 g and 5–6 weeks old were obtained from Japan SLC (Shizuoka, Japan). All experiments were conducted in accordance with the animal experimentation guidelines of University of Toyama and permitted by the Animal Care Committee at the University of Toyama. No side effect due to fucoidan administration was detected throughout the experiments. Mice (each group: $n = 10$) were intra-nasally infected with 5×10^3 plaque-forming units (PFU) of influenza virus in 50 μl phosphate-buffered saline (PBS) on day 0. The fucoidan was given by oral administration at a dose of 1 mg or 5 mg/day twice a day for 14 days from 7 days before virus inoculation until 7 days after inoculation. Control group mice were administered orally with vehicle (distilled water) alone. Lung samples and broncho-alveolar lavage fluids (BALFs) were collected from each group on day 3 to determine the virus yields. Blood samples, BALFs, and faeces were collected from each group on day 14 to evaluate the antibody production. Blood samples were centrifuged at 3000 rpm for 10 min and sera were stored at −20 °C. Lung samples were sonicated for 10 s after adding 1 μl PBS per 1 mg of lung tissue and then centrifuged at 10,000 rpm for 30 min. BALFs were prepared by four washes with 0.8 ml of ice-cold PBS via a tracheal cannula and then centrifuged at 1500 rpm for 10 min. Supernatants obtained from lung and BALFs samples were stored at −80 °C. Faecal extracts were prepared adding PBS at 10 μl per mg of faeces.

2.6. Assay for neutralizing antibody

Neutralizing anti-influenza virus antibody titres of the sera and BALFs were determined using 50% plaque reduction assay. Approximately 100 PFU of virus was mixed with sera at 20–40,000 times dilutions or mixed with BALFs at 1–500 times dilutions, and incubated for 1 h at 37 °C. Each mixture was added onto MDCK cell monolayers in 35-mm dishes. Plaques in each dish were counted after 2 days as described above to measure the residual virus infectivity. The neutralizing antibody titre was considered as the highest dilution of the serum or BALF that reduced the plaque numbers by 50% as compared with no drug control.

2.7. Determination of mucosal IgA levels

ELISA was used for determination of the levels of virus-specific IgA antibodies in BALFs and faeces. Flat-bottom 96-well plates were coated with purified virus at a concentration of 1 μg/ml. After blocking the plates with PBS containing 10% skim milk, different dilutions of BALF were added to the plates and incubated for 1 h at 37 °C. The plates were then reacted with horseradish peroxidase-labelled goat anti-mouse IgA (Santa Cruz Biotechnology, Santa Cruz, CA, USA). After washing, the substrate solution (0.4 mg/ml *O*-phenylendiamine) containing 10 μl/ml H_2O_2 was added. After 20 min to 25 min incubation at room temperature, the reaction was stopped by adding 4 N H_2SO_4 and absorbance was measured at 490 nm on a microplate reader (Spectra rainbow, Tecan Japan Co., Ltd., Kanagawa, Japan).

2.8. Statistics

The effects of the fucoidan were analysed by one-way analysis of variance (ANOVA) and correction for multiple comparisons was done by Turkey's multiple-comparison test. A p value of less than 0.05 was taken as significant.

3. Results

3.1. Preliminary data

Preliminary results characterizing purified fucoidan of this study were presented earlier by Lee et al. (2004). The polysaccharide (M_w ~9 kDa) contained 37.9% of total sugars (mainly fucose and galactose with nearly equal ratio), 1.9% of uronic acids, 10.4% of sulphur in sulphate semi-esters and no proteins. Native and desulphated fucoidans were submitted to methylation analysis led to structural conclusions: (a) desulphated fucoidan contained non-reducing end fucose and galactose, 1,3- and 1,4-linked fucose, and 1,3-, 1,4-, and 1,6-linked galactose; (b) sulphate groups were found at 2-position of Fuc*p* residues and 3- or 6-position of Gal*p* residues. These results pointed to very complex structure of studied heteropolysaccharide that have been later confirmed by other reports of fucoidans isolated from *U. pinnatifida* sporophyll (Hemmingson et al., 2006; Synytsya et al., 2010).

3.2. FT Raman and FTIR spectra

FT Raman and FTIR spectra of native fucoidan **MF** and its derivatives (**DA-MF**, **DS-MF**) are shown in Fig. 1A and B. Broad IR band of **MF** at 3433–3451 cm^{-1} was assigned to HOH/OH stretching vibrations of water and hydroxyls; the next IR band at 1634–1646 cm^{-1} was attributed to the in-plane bending vibration of water. Raman band at 2940–2946 cm^{-1} (with shoulders) as well as several IR bands and shoulders in the region of 2800–3000 cm^{-1} were assigned to CH stretching vibrations in both *O*-acetyl substituents and sugar moieties. Two narrow IR bands at 2923–2928 and 2853–2856 cm^{-1} arose from CH_2 of Gal*p* units. These bands were more pronounced for the derivatives because of removal of *O*-acetyls.

IR band of **MF** at 1738 cm^{-1} (C=O stretching) and IR/Raman band at 1378–1381 cm^{-1} (CH_3 symmetric bending) were assigned to *O*-acetyl groups (Synytsya, Čopíková, Matějka, & Machovič, 2003). Deacetylation led to decrease or disappearing of these bands in the spectra of derivatives. IR/Raman band or shoulder at 1452–1468 cm^{-1} was assigned mainly to scissoring vibration of CH_2 (Gal*p*) with some contribution of antisymmetric bending of CH_3 (Fuc*p*, *O*-acetyls). Raman bands at ~1400 and 1340–1346 cm^{-1} were assigned to in-plane CCH, COH and OCH deformations in pyranoid rings with contribution of CH_2 waging (Gal*p*) and CH_3 symmetric bending (Fuc*p*), respectively (Taleb-Mokhtari, Rahal-Sekkal, & Vergoten, 2003). The envelope of strong to medium IR bands and shoulders at 960–1170 cm^{-1} arose from CO and CC stretching in pyranoid ring and COC stretching of glycosidic bonds (Kačuráková, Capek, Sasinková, Wellner, & Ebringerová, 2000). Intense absorption at this region is common for all polysaccharides.

Raman bands of **MF** at 1270 cm^{-1} (antisymmetric O=S=O stretching), 1072 cm^{-1} (symmetric O=S=O stretching), 836 cm^{-1} (COS bending) and 579 cm^{-1} (symmetric O=S=O bending) are characteristic for sulphate ester groups in polysaccharides (Malfait, van Dael, & van Cauwelaert, 1987; Sekkal & Legrand, 1993). Very intense

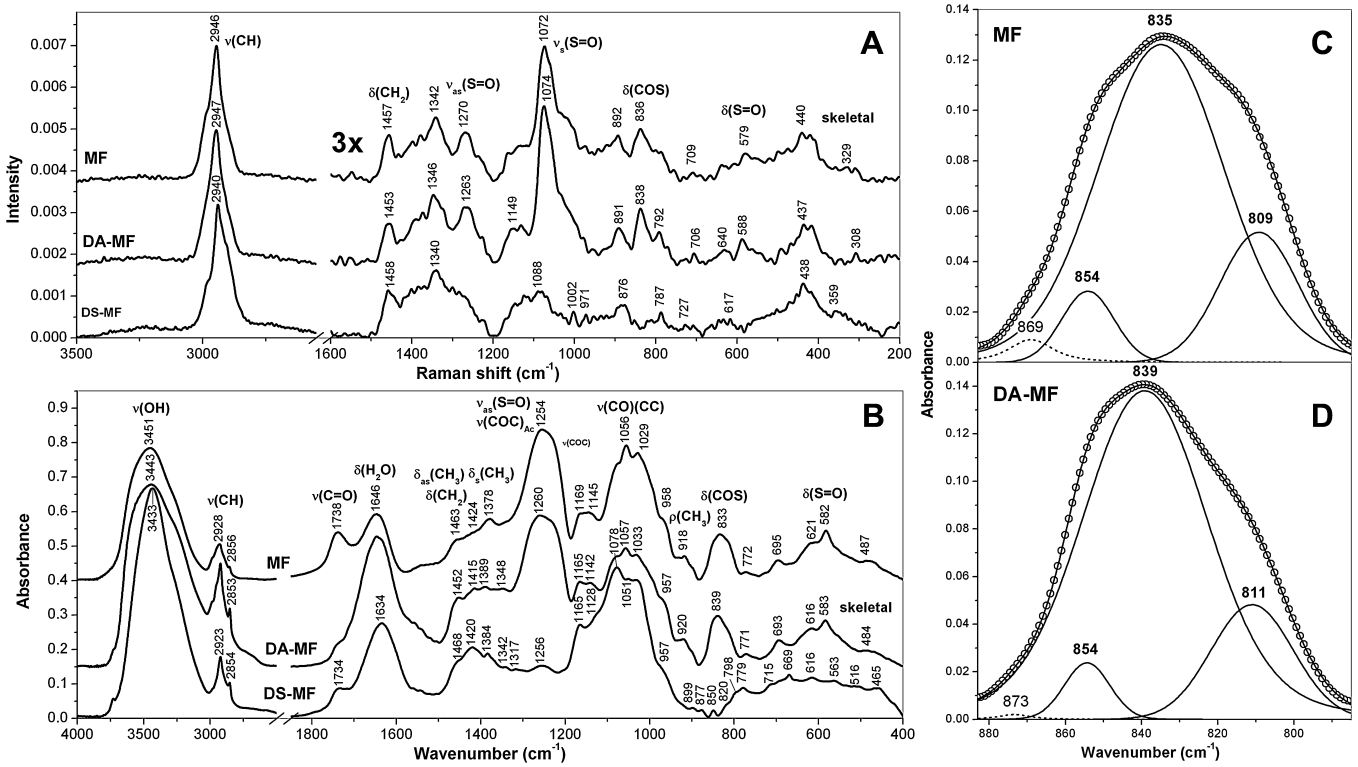

Fig. 1. FT Raman (A) and FTIR (B) spectra of native Mekabu fucoidan (**MF**) and its deacetylated (**DA-MF**) and desulphated (**DS-MF**) derivatives; peak decomposition of FTIR spectra (785–885 cm^{-1}) for **MF** (C) and **DA-MF** (D).

and broad IR band of **MF** at 1254 cm^{-1} was attributed to antisymmetric O═S═O stretching vibration of sulphate esters. This band is typical for sulphated polysaccharides (carrageenans, agar etc.) and was used as a marker of sulphation (Pereira, Amado, Critchley, van de Velde, & Ribeiro-Claro, 2009). However, it has a contribution of COC stretching vibration of *O*-acetyls. Deacetylation led to the shift of the broad sulphate band to 1260 cm^{-1} (**DA-MF**) because of removal of the *O*-acetyl component; band of reminder esters in **DS-MF** was observed at 1256 cm^{-1}. Other IR bands of sulphates were found at 621 and 582 cm^{-1}. These bands were attributed to the antisymmetric and symmetric O═S═O deformations (Sekkal & Legrand, 1993). The band at 833 cm^{-1} was assigned to equatorial C2—O—S or C3—O—S bending vibrations (Chopin & Whalen, 1993; Pereira et al., 2009; Qiu, Amarasekara, & Doctor, 2006; Sekkal & Legrand, 1993), while the shoulders at ~811 and ~854 cm^{-1} could be assigned to bending of primary C6—O—S and axial C4—O—S, respectively. For both **MF** and **DA-MF**, peak decomposition of FTIR spectra in the region of 783–883 cm^{-1} demonstrated four Voigt components at 809–811 cm^{-1} (C6—O—S), 835–839 cm^{-1} (C2,3—O—S), 854 cm^{-1} (C4—O—S) and 869–873 cm^{-1} (skeletal mode of α-Fuc*p*) (Fig. 1C and D). According to relative areas of the appropriate components, the ratio between primary equatorial, secondary equatorial and secondary axial sulphates should be approximately 0.2:1:0.1. Therefore, equatorial sulphates at C-2 and/or C-3 positions of both types of sugar units predominated in **MF**. Desulphation led to disappearing of all the sulphate vibration bands mentioned above in the spectrum of **DS-MF**.

3.3. Proton and carbon-13 NMR spectra

The ^{1}H and ^{13}C APT NMR spectra of native (**MF**), deacetylated (**DA-MF**) and desulphated (**DS-MF**) Mekabu fucoidans are shown in Fig. 2A and B. Resonance signal assignments based on correlation NMR are summarized in Table 1. The spectra of **MF** have intense proton and carbon resonance signals originated from the α-Fuc*p* and β-Gal*p* units as well as from *O*-Ac substituents. The anomeric resonances (δ 4.5–5.4 for H1, δ 98–107 for C1) were detected for both α- and β-anomers. The signals of pyranoid ring protons and carbons were found at δ 3.2–4.5 and 69–83, respectively; the former region includes CH_2 protons of Gal*p*. Four positive carbon resonances at δ 61.6, 61.8, 66.8 and 67.1 were assigned to CH_2 of Gal*p*; the last two are downfield shifted due to the substitution at C6. The proton and carbon signal of CH_3 in α-Fuc*p* were found at δ 1.1–1.3 and 69–83, respectively. Carbon signals of **MF** at δ 175.3–176.5 (C═O) and δ 20.8–21.6 (CH_3) as well as corresponding proton signals at δ 1.65–2.53 (CH_3) indicate the presence of acetyl ester groups (Jansson, Kenne, & Schweda, 1987; Synytsya et al., 2010). A group of downfield shifted resonances at δ 78–84 were assigned to substituted (glycosylated or esterified) carbons. The region of δ 3.0–6.0 (H1–5 of Fuc*p* and H1–6 of Gal*p*) was used as the reference for calculation of relative areas at δ 0.85–1.60 ppm (H6 of Fuc*p*) and at δ 1.65–2.53 (*O*-Ac). Obtained values confirmed that (a) the Fuc*p* to Gal*p* molar ratio was approximately 1:1 that is in agreement with the monosaccharide compositional analysis (Lee et al., 2004), and (b) the degree of acetylation (*DA*) was ~0.42 mol mol^{-1}.

3.4. Correlation NMR spectra

The ^{1}H, ^{13}C HSQC spectra of **MF**, **DA-MF** and **DS-MF** have several distinctive regions as shown in Fig. 3A–C. The C1/H1 region has two sub-regions assigned to α-Fuc*p* and β-Gal*p* units. The former sub-region of **MF** contains much less pronounced signals then those in the latter one. The spectra of **DA-MF** and **DC-MF** have more intense signals of α-Fuc*p*, so subsequent deacetylation and desulphation led to expansion of α-Fuc*p* residues. Evident shifts of the C1/H1 signals in derived fucoidans indicated the loss of sulphate and/or acetyl ester groups. Three H1/C1 HSQC signals of **MF** at δ 4.98/100.6, 5.02/98.6 and 5.27/100.7 were assigned to α-1,3-Fuc*p*, α-1,4-Fuc*p* and α-1,3-Fuc*p*2S units, respectively. According to the relative intense of the signals, the 1,3-linked α-Fuc*p* predominates

Table 1
Assignments for proton and carbon signals of the native Mekabu fucoidan (**MF**) and its deacetylated (**DA-MF**) and desulphated (**DF-MF**) derivatives.

Sample	Unit	C1/H1	C2/H2	C3/H3	C4/H4	C5/H5	C6/H6	C=O	CH_3
MF	→6)-β-Gal*p*-(1→	4.60	3.44	3.67	4.04	3.97	3.94		
		102.2	70.5	69.8	69.1	73.7	67.1		
	→6)-β-Gal*p*-(1→	4.45	3.56	3.75	3.81	4.08	3.98		
		103.6	69.6	69.9	73.8	71.4	66.8		
	→6)-β-Gal*p*-(1→	4.49	3.53	3.70	3.97	4.02	3.94		
		105.0	70.7	69.8	73.6	71.2	67.1		
	→6)-β-Gal*p*3S-(1→	4.63	3.56	4.27	4.19	3.97	3.94		
		103.4	70.8	80.9	67.5	73.7	67.1		
	→4)-β-Gal*p*3S-(1→	4.61	3.63	4.24	4.35	3.54	3.64		
		104.8	70.0	80.7	76.6	75.3	61.6		
	→6)-β-Gal*p*2,4diAc3S-(1→	4.85	4.97	4.60	5.52	4.08	3.99		2·01
		103.1	70.9	76.0	69.5	67.7	66.8	174·0	21·2
									2·08
								173·3	20.8
	→6)-β-Gal*p*3S4Ac-(1→	4.69	3.67	4.39	5.52	4.08	3.99		2·08
		104.8	69.8	78.3	69.5	67.7	66.8	173·3	20.8
	→6)-β-Gal*p*2Ac3S-(1→	4.75	4.97	4.43	4.19	3.94	3.98		2·01
		103.1	70.9	78.4	67.5	73.6	66.8	174·0	21·2
	β-Gal*p*di2Ac,3S-(1→	4.72	4.92	4.45	4.23	3.63	3.68		2·10
		103.3	70.7	76.4	67.5	75.2	61.8	174·5	21·3
	α-Fuc*p*3S-(1→3	4.98	3.94	4.52	3.66	4.33	1.15		
		98.6	67.2	80.5	69.8	67.9	16.4		
	α-Fuc*p*-(1→3	5.02	3.95	4.02	3.77	4.28	1.21		
		96.6	67.2	71.2	68.7	67.6	16.7		
	α-Fuc*p*-(1→4	5.21	3.71	3.97	3.94	4.18	1.13		
		100.8	69.7	69.3	73.6	67.5	16.2		
	→3)-α-Fuc*p*2S-(1→	5.27	4.27	3.96	3.78	4.33	1.19		
		98.7	76.3	73.7	68.6	67.9	16.7		
	→3)-α-Fuc*p*2S-(1→	5.27	4.27	3.96	3.78	4.26	1.13		
		98.7	76.3	73.7	68.7	67.5	16.2		
DA-MF	β-Gal*p*3,6diS-(1→	4.61	3.63	4.25	4.23	3.86	4.08		
		104.7	61.8	80.6	67.4	73.0	67.9		
	→3)-β-Gal*p*-(1→	4.64	3.56	3.74	4.12	3.59	3.67		
		103.5	69.8	83.5	69.3	73.5	61.6		
	→6)-β-Gal*p*2Ac3S-(1→	4.61	4.97	4.47	4.24	3.83	3.96		
		102.4	76.2	74.5	67.6	73.4	67.8		
	β-Gal*p*6S-(1→	4.46	3.56	3.64	4.21	3.86	4.08		
		103.7	69.8	69.8	67.4	73.0	67.9		
	α-Fucp3S-(1→	5.00	3.96	4.54	3.96	4.28	1.22		
		98.6	69.7	78.5	73.1	67.6	16.9		
	α-Fuc*p*3S-(1→	5.01	3.82	4.51					
		98.6	70.3	78.5					
	α-Fucp4S-(1→	5.20	3.72	3.98	4.61	4.18	1.13		
		100.9	69.7	69.3	81.8	67.9	16.1		
	α-Fucp4S-(1→	5.18	3.74	3.97	4.78	4.13	1.13		
		101.2	69.8	69.3	78.8	69.2	16.1		
	→3)-α-Fuc*p*-(1→	4.98	3.96	4.18	3.98	4.24	1.16		
		101.4	69.7	76.2	73.1	67.3	16.1		
	→4)-α-Fuc*p*-(1→	4.99	3.74	3.88	4.03	4.29	1.27		
		101.7	68.7	69.4	79.9	67.4	16.4		
	→3)-α-Fuc*p*2S-(1→	5.40	4.38	4.26					
		99.9	78.6	76.3					
	→3)-α-Fucp2,4S-(1→	5.30	4.46	4.35	4.59	4.33	1.15		
		98.5	78.7	76.6	81.7	67.8	16.6		
DS-MF									
A	→6)-β-Gal*p*-(1→	4.40	3.47	3.61	3.89	3.84	3.84; 3.98		
		104.1	71.4	73.3	69.4	74.4	70.2		
tA	β-Gal*p*-(1→6	4.42	3.54	3.71	4.09	3.88	3.76		
		104.1	71.9	73.8	69.3	74.2	61.6		
A′	→3,6)-β-Gal*p*-(1→	4.58	3.69	3.74	4.10	3.84	3.84; 3.96		
		104.7	70.9	83.0	69.2	74.4	70.2		
B	→4)-β-Gal*p*-(1→	4.50	3.51	3.58	4.10	3.69	3.83; 3.87		
		104.9	71.9	73.2	78.5	73.7	61.4		
B′	→4,6)-β-Gal*p*-(1→	4.54	3.65	3.58	4.14	3.84	3.84; 3.98		
		104.8	71.9	73.2	79.2	74.4	70.6		
C	→3)-β-Gal*p*-(1→	4.58	3.70	3.74	4.07	3.60	3.74		
		104.7	70.9	83.0	69.1	75.8	61.6		
D	→3)-α-Fuc*p*-(1→3	5.03	3.86	3.94	4.03	4.23	1.14		
		96.2	67.1	75.4	68.4	67.2	16.4		
D′	→3)-α-Fuc*p*-(1→3	5.01	3.84	3.97	3.90	4.20	1.17		
		96.2	67.3	75.4	69.3	67.7	16.3		
tD	α-Fuc*p*-(1→3	5.13	3.74	3.88	3.81	4.13	1.12		
		101.6	68.7	69.2	72.9	67.7	16.1		
E	→4)-α-Fuc*p*-(1→3	5.08	3.75	3.97	4.01	4.32	1.27		
		96.0	68.7	69.1	80.0	67.2	16.4		

Table 1 (*Continued*)

Sample	Unit	C1/H1	C2/H2	C3/H3	C4/H4	C5/H5	C6/H6	C=O	CH_3
tE	α-Fuc*p*-(1→4	4.89	3.83	3.88	3.74	4.14	1.13		
		99.1	67.6	69.2	69.8	67.7	16.1		
tE′	α-Fuc*p*-(1→4	4.99	3.72	3.88	3.82	4.30	1.26		
		101.6	68.7	69.2	72.9	67.7	16.1		

in the native polysaccharide, and its smaller fraction is sulphated at C2; the 1,4-linked α-Fuc*p* is less pronounced. Next four H1/C1 signals at δ 4.60/104.2, 4.63/105.4, C1 4.49/105.7 and 4.85/105.1 were assigned to β-Gal*p* units. The H2/C1 HMBC peaks of β-Gal*p* units (not shown) were found at δ 4.95–4.98/105.1 (C2-*O*Ac), 3.53–3.57/105.6 and 3.56/105.1 (C2-unsubstituted).

Parts of the ^{1}H, ^{13}C HSQC, HMBC and ^{1}H, ^{1}H ROESY spectra of **MF** relating to *O*-acetyl substituents are shown in Fig. 4. Several HSQC signals of *O*-acetylated H/C were found at δ 5.52/69.5 (axial C4HOAc), δ 4.92–4.97/70.8 (equatorial C2HOAc) and δ 4.92–4.97/75.9 (equatorial C3HOAc). All these signals indicated *O*-acetylated β-Gal*p* units. The CH_3 protons in *O*-acetyls demonstrated NOE correlation with the mentioned proton resonances; other NOE correspond rather to CHOAc, CH_2OR and/or CH_2OH in the same substituted units than to inter-unit interactions via acetyls. An exception is the weak NOE signal at δ 4.12/2.10 that could be assigned to CH_3 of the acetyl in terminal 2-diacetyl-3-sulphate-β-1,3-Gal*p* unit and H4 of neighbour non-acetylated β-1,3-Gal*p* unit and (Table 1). Several weak HSQC signals of remaining acetylated H/C were found at δ 4.91–4.97/76.4 and δ 4.76–4.79/78.8 (equatorial C3HOAc) for **DA-MF** and at δ 5.23/71.7 (uncertain location) and δ 4.87/75.9 (equatorial C3HOAc) for **DS-MF** (Fig. 2).

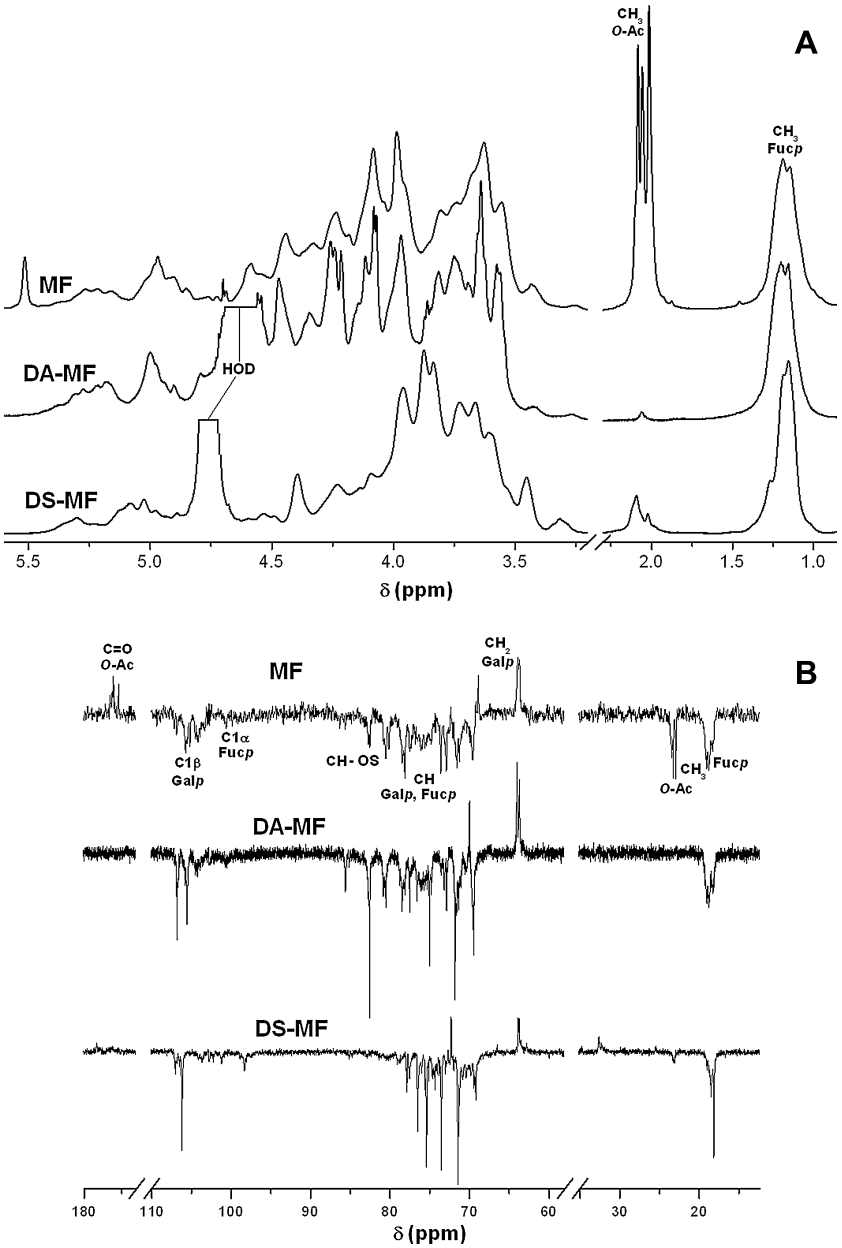

Fig. 2. ^{1}H NMR (A) and ^{13}C APT NMR (B) spectra of native Mekabu fucoidan (**MF**) and its deacetylated (**DA-MF**) and desulphated (**DS-MF**) derivatives.

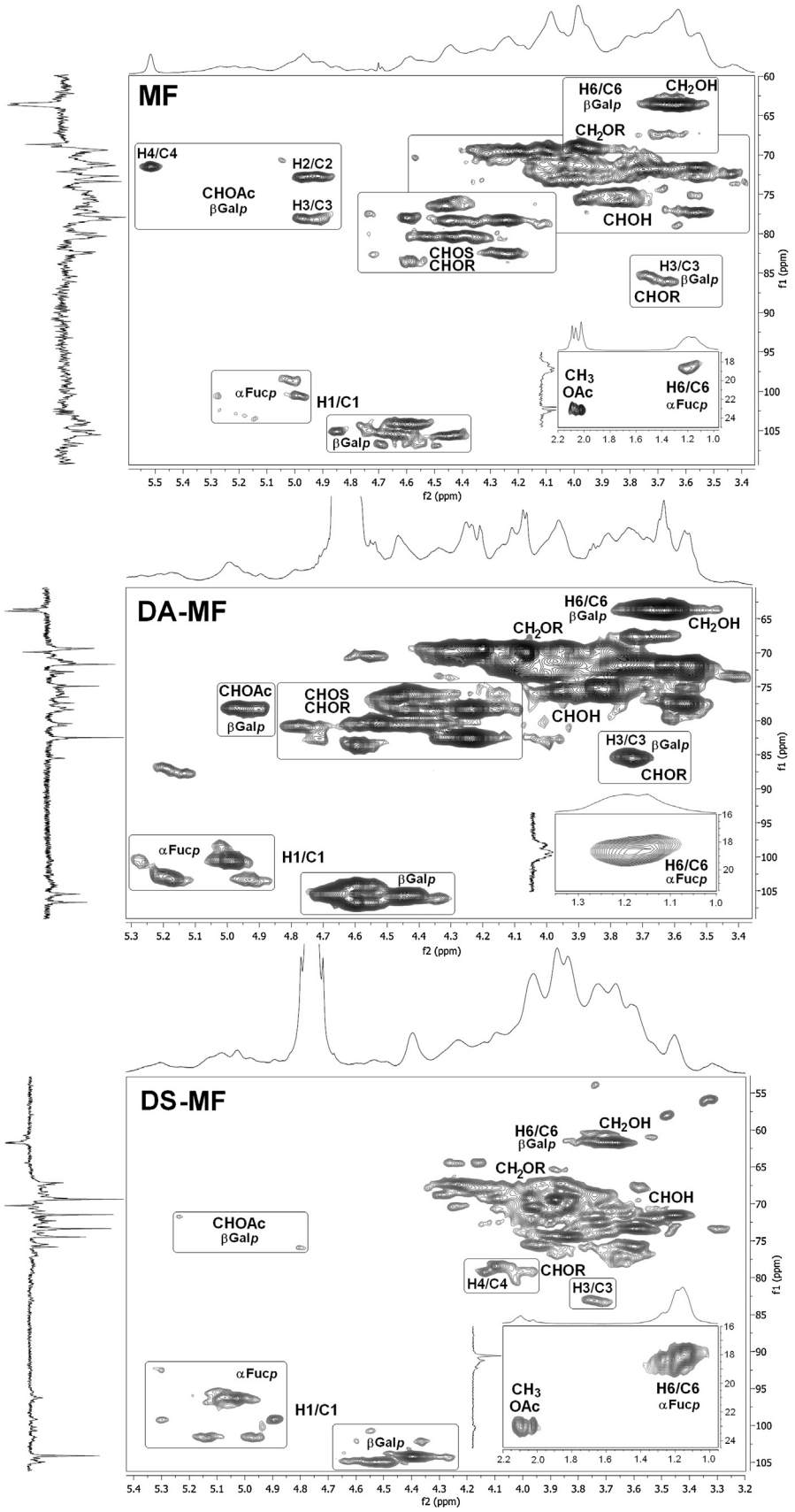

Fig. 3. ^{1}H, ^{13}C HSQC spectra of native Mekabu fucoidan (**MF**) and its deacetylated (**DA-MF**) and desulphated (**DS-MF**) derivatives.

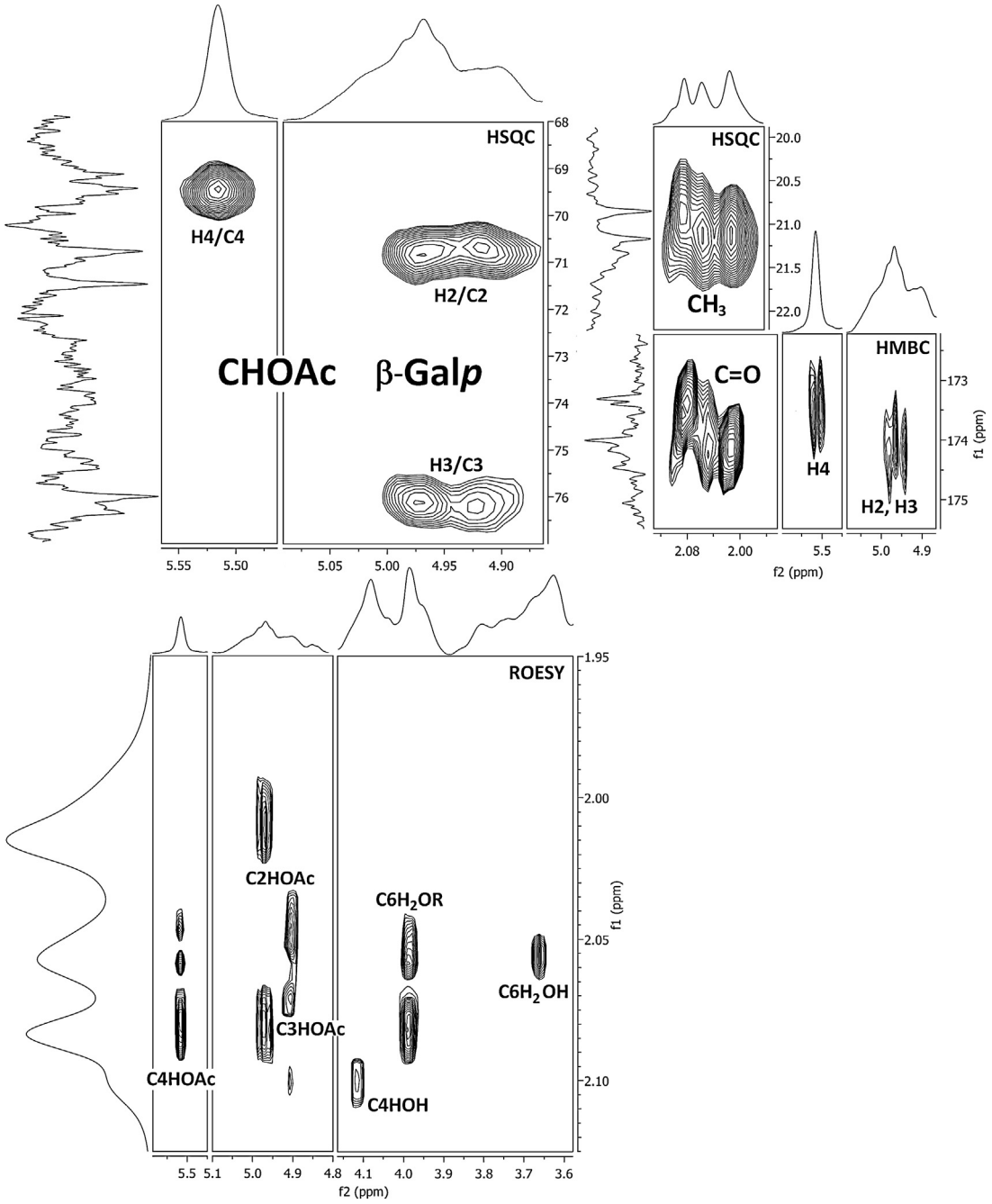

Fig. 4. Parts of the ^{1}H, ^{13}C HSQC, HMBC (top) and ^{1}H, ^{1}H ROESY (bottom) spectra of native Mekabu fucoidan (**MF**) relating to *O*-acetyl substituents of β-Gal*p* units.

It is evident that many significant changes in the intensities and positions of the resonance signals of **DA-MF** and **DS-MF** were caused by deacetylation and/or desulphation of the native polysaccharide **MF**. It is known from the literature devoted to NMR spectra of fucoidans (Bilan et al., 2004, 2002; Synytsya et al., 2010) that *O*-acetylation leads to significant downfield shift of the proton signal ($\Delta\delta$ ~1.2–1.4), while the carbon signal moves downfield slightly ($\Delta\delta$ ~1–2). By contrast, *O*-sulphatation leads to less pronounced downfield shift of the proton signal ($\Delta\delta$ ~0.6–1.0) and marked downfield shift of the carbon signal ($\Delta\delta$ ~6–10). These differences can be used for discrimination of these two types of esters by NMR. However, in the case of Mekabu fucoidan, the situation is complicated by possible presence of several ester substituents per a unit. The problem is commonly solved by removing of the esters. Based on these assumptions and signal assignments for deesterified fucoidans, several acetylated and/or sulphated as well as non-esterified 1,3-, 1.4- and/or 1.6-linked β-Gal*p* units were identified in native fucoidan (Table 1).

The spectra of **DA-MF** and **DS-MF** demonstrated significant changes in the position of signals due to removal of acetyl and/or sulphate esters. The proton and carbon resonances of *O*-acetyls mentioned above are absent or markedly decreased for the derived samples that confirm significant deacetylation in both cases. Three H6/C6 HSQC signals of β-Gal*p* units in **MF** were found at δ 3.64/61.7 (non-substituted), 3.95/67.1 and 3.99/66.8 (C6-substituted); corresponding signals of **DA-MF** and **DS-MF** showed downfield shifts of protons and/or carbons in some cases. The positions of two carbon signals at δ 61.8 and 61.6 (non-substituted C6 of Gal*p*) were slightly changed after chemical treatments, while two signals of **MF** at δ 66.8 and 67.1 (substituted C6 in Gal*p*) were downfield

Table 2
The COSY, TOCSY and ROESY signals $\mathbf{H_x/H_y}$ (δ, ppm) for desulphated Mekabu fucoidan **DS-MF**.

Unit		H_x	H_y/COSY	H_y/TOCSY	H_y/ROESY
A	→6)-β-Gal*p*(1→6	4.40 (**A1**)	3.47 (**A2**)	3.60 (**A3**); 3.88 (**A4**); 3.46 (**A2**)	3.84 (**A5**, **A6**); 3.96 (**A6′**)
tA	β-Gal*p*(1→6	4.42 (**tA1**)	3.54 (**tA2**)	3.71 (**tA′3**); 4.09 (**tA′4**)	3.90 (**A4**); 3.84 (**A5**, **A6**); 3.96 (**A6′**)
A′	→3,6)-β-Gal*p*-(1→	4.58 (**A′1**)	3.70 (**A′2**)	3.75 (**A′3**)	3.75 (**A′3**); 4.11 (**A′4**); 3.88 (**A4**); 4.00 (**A6′**)
B	→4)-β-Gal*p*(1→4	4.50 (**B1**)	3.51 (**B2**)	3.58 (**B3**); 3.83 (**B6**)	4.10 (**B4**); 3.70 (**B5**); 3.89 (**B6**)
B′	→4,6)-β-Gal*p*(1→4	4.54 (**B′1**)	3.65 (**B′2**)	3.58 (**B′3**); 3.64 (**B′2**)	4.14 (**B′4**); 3.84 (**B′5**); 4.11 (**B4**)
C	→3)-β-Gal*p*(1→	4.58 (**C1**)	3.70 (**C2**)	3.75 (**C3**); 3.70 (**C2**)	3.75 (**C3**, **C′3**); 4.11 (**C′4**)
D	→3)-α-Fuc*p*(1→3	5.03 (**D1**)	3.86 (**D2**)	3.95 (**D3**); 3.86 (**D2**); 4.23 (**D5**)	3.94 (**D3**); 3.87 (**D2**); 4.03 (**D4**)
		1.14 (**D6**)	4.23 (**D5**)	4.22 (**D5**)	4.24 (**D5**); 3.97 (**D′3**, **A6′**); 3.89 (**A4**); 3.60 (**A3**); 3.47 (**A2**); 4.40 (**A1**)
D′	→3)-α-Fuc*p*(1→3	5.01 (**D′1**)	3.84 (**D′2**)	3.97 (**D′3**); 3.84 (**D′2**); 3.90 (**D′4**)	3.96 (**D′3**); 3.85 (**D′2**)
		1.17 (**D′6**)	4.20 (**D′5**)	4.20 (**D′**)	4.20 (**D′5**); 3.73 (**tD2**); 3.90 (**D′4**, **tD3**)
tD	α-Fuc*p*(1→3	5.13 (**tD1**)	3.74 (**tD2**)	3.88 (**tD3**); 3.74 (**tD2**); 3.82 (**tD4**)	3.97 (**D′3**); 3.94 (**D3**); 3.89 (**tD3**); 3.74 (**tD2**)
E	→4)-α-Fuc*p*(1→3	5.08 (**E1**)	3.75 (**E2**)	3.97 (**E3**)	3.97 (E3, **D3**); 4.03 (**D4**); 3.86 (**D2**); 3.76 (**E2**)
		1.26 (**E6**)	4.29 (**E5**)	4.28 (**E5**)	4.30 (**E5**); 4.99 (**G1**); 4.02 (**E4**)
tE	α-Fuc*p*(1→4	4.89 (**tE1**)	3.83 (**tE2**)	3.83 (**tE2**)	3.83 (**tE2**); 4.14 (**B′4**); 3.59 (**B′3**)
		1.13 (**E6**)	4.13 (**E5**)	4.14 (**E5**)	4.15 (**E5**); 3.73 (**E4**)
tE′	α-Fuc*p*(1→4	4.99 (**tE′1**)	3.72 (**tE′2**)	3.87 (**tE′3**); 4.31 (**tE′5**); 3.83 (**tE′4**); 3.72 (**tE′2**)	3.96 (**E3**); 3.75 (**E2**); 3.89 (**tE′3**)

shifted to δ 67.9 (**DA-MF**) and to δ 70.2–70.6 (**DS-MF**). Therefore, the shifted signals indicate glycosylation at C6 of some Gal*p* units in **MF**. These units were acetylated and/or sulphated at proximal positions, and subsequent deesterification caused the downfield shifts observed for **DA-MF** and **DS-MF**. The substituted carbon signals of **MF** at δ 78–84 were found in the spectrum of **DA-MF** but absent in the spectrum of **DS-MF**, so they should correspond to sulphated carbons. Three HSQC signals of **DA-MF** at 4.45/78.4, 4.47/76.6 and 4.53/80.5 were assigned to sulphated H/C; these signals are absent in the spectrum of **DS-MF** because of desulphation. Two H6/C6 HSQC peaks of β-Gal*p* units in **DS-MF** were found at δ 3.67–3.74/61.6–61.8 (non-substituted) and 3.84/70.2 (substituted); the next less pronounced peaks at δ 3.74–3.76/83.0 (H3/C3), 4.10/78.5 and 4.14/79.2 (H4/C4) corresponded to β-Gal*p* units glycosylated at C3 and C4 positions, respectively. All these latter units were previously detected by methylation analysis (Lee et al., 2004).

Key intra- and inter-unit COSY, TOCSY and ROESY NMR signals of **DS-MF** are summarized in Table 2. The ROESY signals of internal β-Gal*p* units indicated the presence of three types of mutually connected β-galactans. Sequences of (1→6)-β-galactan (**A**, **tA** and **A′** units) are probably attached to the (1→4)-β-galactan core (**B**, **B′** units) at C-6 positions of **B′**. Similarly, less pronounced linear (1→3)-β-galactan (**C** units) is probably bound to (1→6)-β-galactan at C-6 positions of **A′**. The fragments of linear (1→3)(1→4)-α-fucan (**D**, **D′**, **tD**, **E** and **tE** units) or single α-Fuc*p* (**tE** units) are also bound to (1→4)(1→6)-β-galactan. Resulting structure of **DS-MF** is highly branched complex (1→3)(1→4)-α-fuco-(1→3)(1→4)(1→6)-β-galactan.

3.5. Effects on virus production in avian virus-infected mice

A mouse model of nasal infection was used for the determination of in vivo efficacy of **MF** against avian influenza viruses. Mice were intra-nasally inoculated with a non-lethal dose of H5N3 or H7N2 virus containing 5×10^3 PFU per animal. No death was observed at this viral challenge dose throughout the experiments. Oral administration of **MF** significantly inhibited viral proliferation in the lungs and BALFs compared with the control group at 3d after the infection in a dose-dependent manner (Fig. 5A). At a higher dose (5 mg/day) of **MF**, the mean virus titres of the lungs were reduced by 82% ($p < 0.05$) and 77% ($p < 0.05$) in H5N3- and H7N2-infected mice, respectively as compared with those of the control group (Fig. 5A). Similarly, the mean virus yields of BALFs in H5N3- and H7N2-infected fucoidan groups decreased by 71% and 86% ($p < 0.05$), respectively, as compared with those of control group at a dose of 5 mg/day (Fig. 5A).

3.6. Effects on antibody responses in sera and mucosa

In an attempt to elucidate whether oral administration of **MF** could stimulate systemic and local immune responses in avian virus-infected animals, virus-specific antibody titres in sera, BALFs and faeces were determined on day 14 post-infection. The levels of neutralizing antibody in sera and BALFs are shown in Fig. 5B. The administration of **MF** produced dose-dependently higher antibody titres in the sera and BALFs as compared with those in the control group during the 2 weeks after viral infection. The neutralizing antibody titres of the sera in a higher dose fucoidan group were approximately 2.8 ($p < 0.05$) and 2.1 times ($p < 0.01$) higher in H5N3- and H7N2-infected mice, respectively, than the control group.

Secretory IgA antibody in the mucosa plays a crucial role in suppressing influenza virus replication. To investigate whether the fucoidan affects production of secretory IgA in the mucosa, the levels of IgA in the respiratory organs (BALFs) and the intestine (faeces) were determined by an ELISA assay. As shown in Fig. 5C, the levels of IgA in the BALFs and faeces showed a similar tendency. Fucoidan groups produced higher BALF and faecal levels than those of the control group in both H5N3- and H7N2-infected mice. The IgA levels in BALFs increased 2.4- ($p < 0.05$) and 2.7-times ($p < 0.05$) in H5N3- and H7N2-infected mice, respectively, following the administration of a high dose of **MF**; the increases of IgA levels were also detected in the faeces.

4. Discussion

4.1. Structural patterns of Mekabu fucoidan

Spectroscopic analyses possessed valuable information about structural patterns of native Mekabu fucoidan. It was confirmed that this is highly *O*-acetylated (*DA* ~0.42 mol mol^{-1}) and sulphated fucogalactan containing fucose and galactose units at ca.

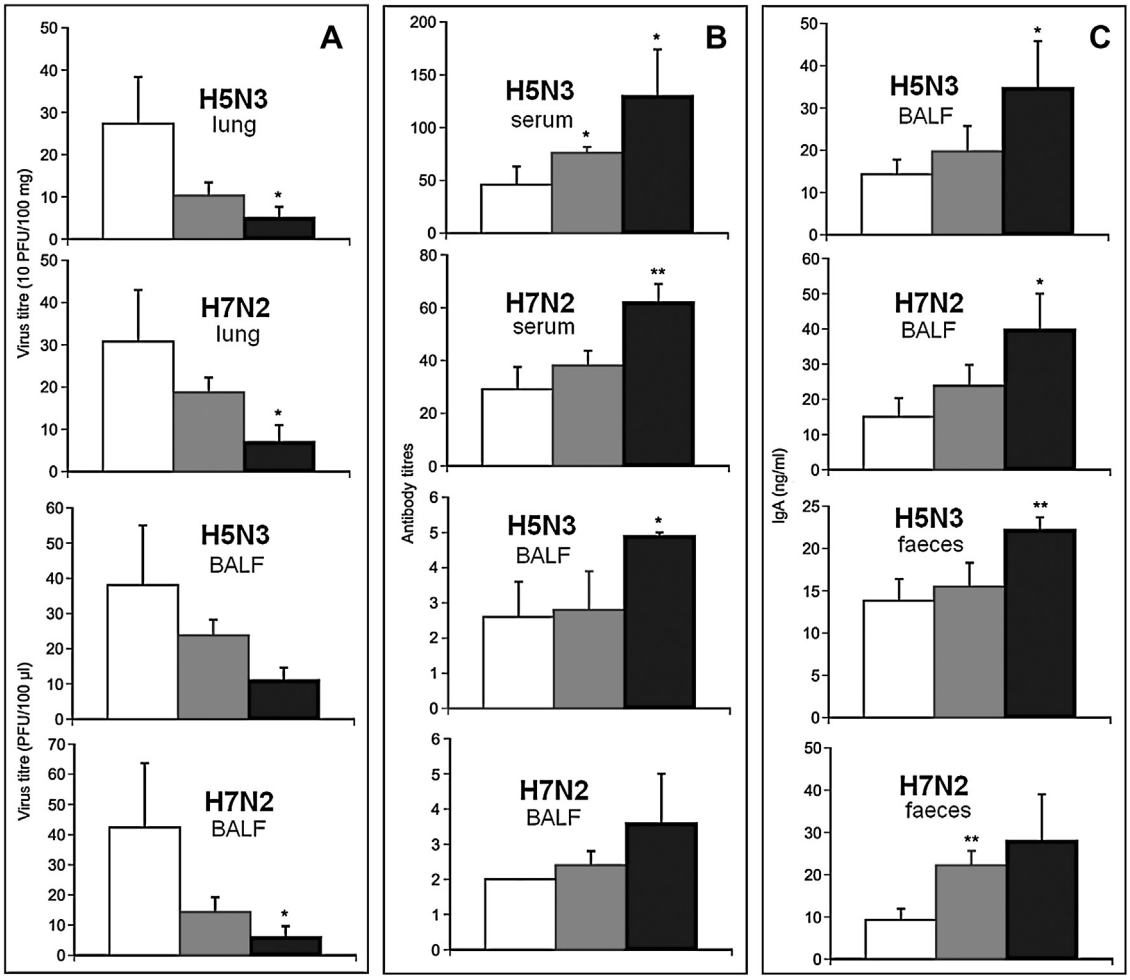

Fig. 5. Effects of oral Mekabu fucoidan (**MF**) on virus yields (A), production of neutralizing antibody (B) and production of avian influenza virus-specific IgA antibody (C) in mice infected with H5N3 or H7N2 avian influenza viruses. Infected mice were administered with distilled water (control) (open column), 1 mg of **MF** (grey column) or 5 mg of **MF** (closed column) (see details in the Experimental part); each value was presented as the mean ± SD; $^{*}p < 0.05$, $^{**}p < 0.01$ versus the control group.

1:1 molar ratio. The β-Gal*p* and α-Fuc*p* units of different linkages were detected; the acetylation/sulphation patterns were quite variable. The resonance signals of α-Fuc*p* in native fucoidan were less pronounced than those of β-Gal*p*, maybe owing to structural and conformation properties of this polysaccharide. Subsequent deacetylation and desulphation, however, led to more pronounced α-Fuc*p* signals in comparison with corresponding β-Gal*p* signals.

NMR analysis of native and derived Mekabu fucoidan confirmed the presence of 1,3-linked α-Fuc*p* and 1,6-linked β-Gal*p* as the main units; terminal and 1,4-linked α-Fuc*p* as well as terminal, 1,3- and 1,4-linked β-Gal*p* were also found, but their signals were less pronounced. These results are in agreement with methylation analysis published earlier (Lee et al., 2004). No uronic acid units were found, so all the carbonyl groups detected (4–5 patterns) are of *O*-acetyls. Sulphation of α-Fuc*p* at C2, C3 and C4 positions was also detected; β-Gal*p* units were sulphated at C3 or C6 and/or acetylated at C2, C3 or C4 positions. Equatorial *O*-acetyls at C2 or C3 seems to be more resistant to the treatment with NH_3OH than axial *O*-acetyls at C4. Correlation NMR analysis (ROESY) of the desulphated and deacetylated polysaccharide determined the relationship between α-fucan and β-galactan fragments. It was found that these fragments are tightly integrated forming highly branched fucogalactan, which have (1→4)-β-galactan core and side chains consisting of α-fucans and other β-galactans.

Galactose-containing sulphated fucoidans of complex structure have been described earlier for some brown algae (Li, Lu, Wei, & Zhao, 2008). For example, *Spatoglossum schroederi* contains a polysaccharide having partially 3-*O*-sulphated (1→4)-β-galactan as the central core (Rocha et al., 2005). About ¼ of these units carried oligosaccharide branches composed of 4-linked α-Fuc*p*-3-sulphate and β-Xyl*p* units. Fucoidan from *Hizikia fusiforme* (fraction F32) contained a fucose-free core composed of alternating sequence of →2)-α-Man*p*(1→ and →4)-β-Glc*p*A(1→ with admixture of →4)-β-Gal*p*(1→, while the side chains containing β-Gal*p*, α-Fuc*p* and/or α-Xyl*p* units were attached to the core (Li, Xin, Sun, & Xu, 2006). Bilan et al. (2010) described three types of sulphated heteropolysaccharides (fucogalactan, fucoglucuronomannan and fucoglucuronan) in the total fucoidan preparation from *Saccharina latissima*. Like in the previous case, all these fucoidans contained fucose-free cores and α-Fuc*p* as single branches. Therefore, different sulphated polysaccharides were found to be minor structural parts of a crude fucoidan preparation. Similarly, fractionation of crude fucoidan from sporophyll of *U. pinnatifida* (Hemmingson et al., 2006) confirmed structural heterogeneity of this polysaccharide; our previous and present investigations also demonstrated the presence of different structural parts (fucan and galactan fragments) in the whole structure of Mekabu fucoidan.

4.2. Antiviral effects of Mekabu fucoidan

In recent years, there have been human cases of highly pathogenic avian influenza viruses reported to WHO (World

Health Organization, 2013a). Although transmission from person-to-person is limited, the virus has the potential to emerge as a source of the next influenza pandemic (Ungchusak et al., 2005). In the previous studies, the Mekabu fucoidan was shown to exert potent action in vivo against the replication of herpes simplex virus type 1 (HSV-1) (Hayashi et al., 2008) and influenza A virus (H1N1 subtype) (Hayashi et al., 2013, 2007). In the present study, we showed that administration of Mekabu fucoidan inhibited the replication of the two subtypes of avian influenza viruses in mice.

The direct antiviral activity of the sulphated seaweed polysaccharides is based on the formation of specific supramolecular complexes (similar to those between cells and viruses), which block virus–cell adhesion and thus (Damonte, Matulewicz, & Cerezo, 2004). Such complexes are stabilized by non-covalent interactions, mainly electrostatic but also hydrophobic and/or polar ones. In this context, several structural prerequisites of antiviral sulphated polysaccharides were defined (Ghosh et al., 2009): (a) degree of sulphatation as well as charge density is the principal factor providing electrostatic interactions; (b) presence of *O*-acetyl groups may support antiviral activity due to hydrophobic and hydrogen bonding interactions; (c) specific positioning of sulphate/acetyl might be also important; (d) molecular weight also influences antiviral activity (smaller molecules more effectively inhibit cell-to-cell spread of viruses). Mekabu fucoidan of this study demonstrate structural properties suitable for potential antiviral activity, i.e. low molecular weight (M_w ~9 kDa), high sulphatation degree (10.4% of sulphur) and significant amount of *O*-acetyls (*DA* ~0.42 mol mol^{-1}). However, the whole structure of this fucoidan was found to be too complex to define which structural features may be responsible for the antiviral effects described above.

When viruses invade the human body, they encounter the host immune responses, which can be typically subdivided into innate and adaptive immunity. One of the former is supported by macrophages, those having a phagocytic ability that contributes to eliminate viruses as an early reduction of the virus load (Didierlaurent, Goulding, & Hussell, 2004). We have previously reported that Mekabu fucoidan enhanced the function of macrophages (Hayashi et al., 2008). NK cells also provide an early line of host defence before antigen-specific immune responses develop (McGill, Heusel, & Legge, 2009), and we also reported that oral administration of Mekabu fucoidan suppressed decreasing NK activity in the immunosuppressed mice (Hayashi et al., 2008). In this study, we investigated the adaptive immunity in avian influenza virus-infected mice. It was found that consecutive oral administration of the fucoidan suppressed the viral replication and enhanced the production of neutralizing antibody and mucosal IgA. These findings suggested the potential of fucoidan in enhancing innate immunity including NK and macrophage activities. In addition, a higher proportion of large B cells (plasma cells) were observed in the splenic B cell population after treatment with MF (Hayashi et al., 2008). This result might imply that the fucoidan induces the differentiation of B cells, the events bringing about antibody production. Actually, in the present study, we indicated increasing avian virus-specific antibody in mice.

Among adaptive immune mechanisms, it is important to induce mucosal immunity since influenza virus enters its host through a mucosal surface (Tamura & Kurata, 2004). As shown in Fig. 5C, Mekabu fucoidan produced 1.4–3 times more IgA levels in the mucosa than those in the control animals. These immune responses caused by the fucoidan might be due to its stimulation of innate and adaptive immune defence functions, and contribute to the relief of the symptoms of influenza virus infection. In all, Mekabu fucoidan, a sulphated polysaccharide prepared from *U. pinnatifida*, showed favourable effects in the control of not only seasonal influenza virus but also avian influenza virus infections.

Acknowledgments

This article was supported by the project No. CEZ:MSM6046137305 of the Ministry of Education of the Czech Republic and by the Institute of Chemical Technology in Prague, financial Support from Specific University Research (MSMT No. 20/2013).

References

Bilan, M. I., Grachev, A. A., Shashkov, A. S., Kelly, M., Sanderson, C. J., Nifantiev, N. E., et al. (2010). Further studies on the composition and structure of a fucoidan preparation from the brown alga *Saccharina latissima*. *Carbohydrate Research*, *345*, 2038–2047.

Bilan, M. I., Grachev, A. A., Ustuzhanina, N. E., Shashkov, A. S., Nifantiev, N. E., & Usov, A. I. (2002). Structure of a fucoidan from the brown seaweed *Fucus evanescens* C. Ag. *Carbohydrate Research*, *337*, 719–730.

Bilan, M. I., Grachev, A. A., Ustuzhanina, N. E., Shashkov, A. S., Nifantiev, N. E., & Usov, A. I. (2004). A highly regular fraction of a fucoidan from the brown seaweed *Fucus distichus* L. *Carbohydrate Research*, *339*, 511–517.

Boo, H. J., Hyun, J. H., Kim, S. C., Kang, J. I., Kim, M. K., Kim, S. Y., et al. (2011). Fucoidan from *Undaria pinnatifida* induces apoptosis in A549 human lung carcinoma cells. *Phytotherapy Research*, *25*, 1082–1086.

Chizhov, A. O., Dell, A., Morris, H. R., Haslam, S. M., McDowell, R. A., Shashkov, A. S., et al. (1999). A study of fucoidan from the brown seaweed *Chorda filum*. *Carbohydrate Research*, *320*, 108–119.

Chopin, T., & Whalen, E. (1993). A new and rapid method for carrageenan identification by FT IR diffuse reflectance spectroscopy directly on dried, ground algal material. *Carbohydrate Research*, *246*, 51–59.

Damonte, E. B., Matulewicz, M. C., & Cerezo, A. S. (2004). Sulfated seaweed polysaccharides as antiviral agents. *Current Medicinal Chemistry*, *11*, 2399–2419.

Didierlaurent, A., Goulding, J., & Hussell, T. (2004). The impact of successive infections on the lung microenvironment. *Immunology*, *122*, 457–465.

Fitton, J. H. (2011). Therapies from fucoidan; multifunctional marine polymers. *Marine Drugs*, *9*, 1731–1760.

Ghosh, T., Chattopadhyay, K., Marschall, M., Karmakar, P., Mandal, P., & Ray, B. (2009). Focus on antivirally active sulfated polysaccharides: From structure–activity analysis to clinical evaluation. *Glycobiology*, *19*, 2–15.

Hayashi, K., Lee, J. B., Nakano, T., & Hayashi, T. (2013). Anti-influenza A virus characteristics of a fucoidan from sporophyll of *Undaria pinnatifida* in mice with normal and compromised immunity. *Microbes and Infection*, *15*, 302–309.

Hayashi, K., Nakano, T., Hashimoto, M., Kanekiyo, K., & Hayashi, T. (2008). Defensive effects of a fucoidan from brown alga *Undaria pinnatifida* against herpes simplex virus infection. *International Immunopharmacology*, *8*, 109–116.

Hayashi, T., Hayashi, K., Kanekiyo, K., Ohta, Y., Lee, J. B., Hashimoto, M., et al. (2007). Promising antiviral glycol-molecules from an edible alga. In P. F. Torrence (Ed.), *Combating the threat of pandemic influenza: Drug discovery approaches* (pp. 116–132). New York: John Wiley & Sons Inc.

Hemmingson, J. A., Falshaw, R., Furneaux, R. H., & Thompson, K. (2006). Structure and antiviral activity of the galactofucan sulfates extracted from *Undaria pinnatifida* (Phaeophyta). *Journal of Applied Phycology*, *18*, 185–193.

Jansson, P.-E., Kenne, L., & Schweda, E. (1987). Nuclear magnetic resonance and conformational studies on monoacetylated methyl D-gluco- and D-galacto-pyranosides. *Journal of Chemical Society, Perkin Transactions*, *1*, 377–383.

Kačuráková, M., Capek, P., Sasinková, V., Wellner, N., & Ebringerová, A. (2000). FT-IR study of plant cell wall model compounds: pectic polysaccharides and hemicelluloses. *Carbohydrate Polymers*, *43*, 195–203.

Katsube, T., Yamasaki, Y., Iwamoto, M., & Oka, S. (2003). Hyaluronidase-inhibiting polysaccharide isolated and purified from hot water extract of sporophyll of *Undaria pinnatifida*. *Food Science and Technology Research*, *9*, 25–29.

Kim, K. J., Yoon, K. Y., & Lee, B. Y. (2012). Low molecular weight fucoidan from the sporophyll of *Undaria pinnatifida* suppresses inflammation by promoting the inhibition of mitogen-activated protein kinases and oxidative stress in RAW264.7 cells. *Fitoterapia*, *83*, 1628–1635.

Kim, W. J., Koo, Y. K., Jung, M. K., Moon, H. R., Kim, S. M., Synytsya, A., et al. (2010). Anticoagulating activities of low-molecular weight fuco-oligosaccharides prepared by enzymatic digestion of fucoidan from the sporophyll of Korean *Undaria pinnatifida*. *Archives Pharmacal Research*, *33*, 125–131.

Lee, J. B., Hayashi, K., Hashimoto, M., Nakano, T., & Hayashi, T. (2004). Novel antiviral fucoidan from sporophyll of *Undaria pinnatifida* (Mekabu). *Chemical and Pharmaceutical Bulletin*, *52*, 1091–1094.

Lee, Y. K., Lim, D. J., Lee, Y. H., & Park, Y. I. (2006). Variation in fucoidan contents and monosaccharide compositions of Korean *Undaria pinnatifida* (Harvey) suringar (Phaeophyta). *Algae*, *21*, 157–160.

Li, B., Lu, F., Wei, X., & Zhao, R. (2008). Fucoidan: structure and bioactivity. *Molecules*, *13*, 1671–1695.

Li, B., Xin, J. W., Sun, J. L., & Xu, S. Y. (2006). Structural investigation of a fucoidan containing a fucose-free core from the brown seaweed *Hizikia fusiforme*. *Carbohydrate Research*, *341*, 1135–1146.

Liu, F., Wang, J., Chang, A. K., Liu, B., Yang, L., Li, Q., et al. (2012). Fucoidan extract derived from *Undaria pinnatifida* inhibits angiogenesis by human umbilical vein endothelial cells. *Phytomedicine*, *19*, 797–803.

Mak, W., Hamid, N., Liu, T., Lu, J., & White, W. L. (2013). Fucoidan from New Zealand *Undaria pinnatifida*: monthly variations and determination of antioxidant activities. *Carbohydrate Polymers*, *95*, 606–614.

Malfait, T., van Dael, H., & van Cauwelaert, F. (1987). Raman spectroscopic analysis of the sodium salt of kappa-carrageenan and related compounds in solution. *Carbohydrate Research*, *163*, 9–14.

Maruyama, H., Tamauchi, H., Hashimoto, M., & Nakano, T. (2003). Antitumor activity and immune response of Mekabu fucoidan extracted from sporophyll of *Undaria pinnatifida*. *In Vivo*, *17*, 245–249.

Maruyama, H., Tamauchi, H., Hashimoto, M., & Nakano, T. (2005). Suppression of Th2 immune responses by mekabu fucoidan from *Undaria pinnatifida* sporophylls. *International Archive of Allergy and Immunology*, *137*, 289–294.

Maruyama, H., Tamauchi, H., Iizuka, M., & Nakano, T. (2006). The role of NK cells in antitumor activity of dietary fucoidan from *Undoria pinnatifida* sporophylls (Mekabu). *Planta Medica*, *72*, 1415–1417.

Maruyama, H., Tanaka, M., Hashimoto, M., Inoue, M., & Sasahara, T. (2007). The suppressive effect of Mekabu fucoidan on an attachment of *Cryptosporidium parvum* oocysts to the intestinal epithelial cells in neonatal mice. *Life Science*, *80*, 775–781.

Maruyama, H., Suzuki, K., Miyai, S., & Ohtsuki, K. (2008). Characterization of meFucoidan as a selective inhibitor for secretory phospholipase A2-IIA and the phosphorylation of meFucoidan-binding proteins by A-kinase in vitro. *Biological and Pharmaceutical Bulletin*, *31*, 714–718.

McGill, J., Heusel, J. W., & Legge, K. L. (2009). Innate immune control and regulation of influenza virus infections. *Journal of Leukocyte Biology*, *86*, 803–812.

Nagasawa, K., Inoue, Y., & Kamata, T. (1977). Solvolytic desulfation of glycosaminoglycuronan sulfates with dimethyl sulfoxide containing water or methanol. *Carbohydrate Research*, *58*, 47–55.

Negishi, H., Mori, M., Mori, H., & Yamori, Y. (2013). Supplementation of elderly Japanese men and women with fucoidan from seaweed increases immune response to seasonal influenza vaccination. *Journal of Nutrition*, *143*, 1794–1798.

Pereira, L., Amado, A. M., Critchley, A. T., van de Velde, F., & Ribeiro-Claro, P. J. A. (2009). Identification of selected seaweed polysaccharides (phycocolloids) by vibrational spectroscopy (FTIR-ATR and FT-Raman). *Food Hydrocolloids*, *23*, 1903–1909.

Pielesz, A., Biniaś, W., & Paluch, J. (2011). Mild acid hydrolysis of fucoidan: characterization by electrophoresis and FT-Raman spectroscopy. *Carbohydrate Research*, *346*, 1937–1944.

Qiu, X., Amarasekara, A., & Doctor, V. (2006). Effect of oversulfation on the chemical and biological properties of fucoidan. *Carbohydrate Polymers*, *63*, 224–228.

Rocha, H. A., Moraes, F. A., Trindade, E. S., Franco, C. R., Torquato, R. J., Veiga, S. S., et al. (2005). Structural and hemostatic activities of a sulfated galactofucan from the brown alga *Spatoglossum schroederi*. An ideal antithrombotic agent? *Journal of Biological Chemistry*, *280*(50), 41278–41288.

Sekkal, M., & Legrand, P. (1993). A spectroscopic investigation of the carrageenans and agar in the 1500–100 cm^{-1} spectral range. *Spectrochimica Acta*, *49A*, 209–221.

Synytsya, A., Čopíková, J., Matějka, P., & Machovič, V. (2003). Fourier transformed Raman and infrared spectroscopy of pectins. *Carbohydrate Polymers*, *54*, 97–106.

Synytsya, A., Kim, W. J., Kim, S. M., Pohl, R., Synytsya, Al., Kvasnička, F., et al. (2010). Structure and antitumour activity of fucoidan isolated from sporophyll of Korean brown seaweed *Undaria pinnatifida*. *Carbohydrate Polymers*, *81*, 41–48.

Taboada, M. C., Millán, R., & Miguez, M. I. (2013). Nutritional value of the marine algae wakame (*Undaria pinnatifida*) and nori (*Porphyra purpurea*) as food supplements. *Journal of Applied Phycology*, *25*(5), 1271–1276.

Taleb-Mokhtari, I. N., Rahal-Sekkal, M., & Vergoten, G. (2003). Modified UBFF calculations of the alpha-L-fucopyranose molecule in the crystalline state. *Spectrochimica Acta. Part A: Molecular and Biomolecular Spectroscopy*, *59*(3), 607–616.

Tamura, S., & Kurata, T. (2004). Defense mechanisms against influenza virus infection in the respiratory tract mucosa. *Japanese Journal of Infectious Diseases*, *57*, 236–247.

Ungchusak, K., Auewarakul, P., Dowell, S. F., Kitphati, R., Auwanit, W., Puthavathana, P., et al. (2005). Probable person-to-person transmission of avian influenza A (H5N1). *New England Journal of Medicine*, *352*, 333–340.

World Health Organization. (2010). In R. Adrienne (Ed.), *Evolution of a pandemic: A(H1N1) 2009, April 2009–August 2010*.

World Health Organization. (2013a). *Number of confirmed human cases for avian influenza A(H7N9) reported to WHO*. http://www.who.int/influenza/human_animal_interface/influenza_h7n9/Data_Reports/en/index.html (cited 07.05.13)

World Health Organization. (2013b). *Cumulative number of confirmed human cases for avian influenza A (H5N1) reported to WHO, 2003–2013*. http://www.who.int/influenza/human_animal_interface/EN_GIP_20130426CumulativCumulati5N1cases.pdf (cited 16.05.13)

Yang, C., Chung, D., Shin, I. S., Lee, H., Kim, J., Lee, Y., et al. (2008). Effects of molecular weight and hydrolysis conditions on anticancer activity of fucoidans from sporophyll of *Undaria pinnatifida*. *International Journal of Biological Macromolecules*, *43*, 433–437.

Yang, L., Wang, P., Wang, H., Li, Q., Teng, H., Liu, Z., et al. (2013). Fucoidan derived from *Undaria pinnatifida* induces apoptosis in human hepatocellular carcinoma SMMC-7721 cells via the ROS-mediated mitochondrial pathway. *Marine Drugs*, *11*, 1961–1976.

Yoo, Y. C., Kim, W. J., Kim, S. Y., Kim, S. M., Chung, M. K., Park, J. W., et al. (2007). Immunomodulating activity of a fucoidan isolated from Korean *Undaria pinnatifida* sporophyll. *Algae*, *22*, 333–338.